

STUDY OF THE AERODYNAMIC INSTABILITIES IN AN AXIAL FLOW COMPRESSOR USING 3D-1D CODES COUPLING APPROACH.

F. de Crécy – G. Després – G. Ngo Boum – F. Leboeuf

Laboratory of Fluid Mechanic and Acoustics, UMR CNRS 5509, Ecole Centrale de Lyon,
University of Lyon, INSA de Lyon

florence.de-crecy@ec-lyon.fr, guillaume.despres@ec-lyon.fr, ghislaine.ngo-boum@ec-lyon.fr,
francis.leboeuf@ec-lyon.fr

ABSTRACT

This article presents a coupling method between 1D and 3D CFD codes developed in order to simulate a surge cycle of a compressor stage. The idea is to use 3D URANS code to compute the aerodynamic field of the compressor and to have 1D code and pressure loss correlations to model the surrounding test bench facility. Thus, an unsteady aerodynamic field of the compressor during a surge cycle can be obtained with reasonable computation costs.

Coupling methodology has been tested on an academic air flow configuration in order to validate the model. Analysis focuses on the quality of information transmission and the reliability of the simulation model in case of mass flow reversal.

In a second step, the simulation model is used to study instabilities in one stage of a highly loaded axial flow compressor. Several surge cycles are simulated and aerodynamic fields are analysed during surge and at minimum mass flow.

NOMENCLATURE

| | |
|---------|--|
| ρ | density |
| V | velocity |
| P_s | static pressure |
| E_t | total energy |
| T_s | static temperature |
| a | sound velocity |
| Q | mass flow rate |
| x,y,z | x is the direction along the 1D flow and the axial direction of the compressor |
| tot | subscript for stagnation pressure or stagnation temperature |
| 3D | subscript for values issued from 3D code |
| 1D | subscript for values issued from 1D code |

INTRODUCTION

A compressor drives the fluid from low pressure zone toward high pressure zones, and that is opposite to the natural behaviour of the fluid. Energy is provided to fluid by forcing a movement of blades. If flow losses are high enough so that compressor blade forces cannot block any more the movement of fluid towards low pressure regions, the mass flow is reversed. Then, the compressor operating point follows approximately a loss line and moves to a region where it can work as a compressor again and where the fluid flows again from inlet to outlet of the compressor. This axial wave of mass flow and pressure is called surge. For a constant rotation speed of the compressor rotor, this instability limits the operating range of the compressor on low mass flow side where the pressure ratio is also the highest. Without other external action for instance on the throttle valve, this cycle on the compressor performance map may repeat many times.

Surge has significant impact on blade vibrations. Experimental data on surge show material damages on blades. During a surge cycle, loading of blades change from stall to reversed flow very quickly (Di Mare, 2009). Blades see a mechanical shock which should be well-known to properly predict their forced response. It is, therefore, necessary to calculate 3D aerodynamic damping under surge and that is why a 3D unsteady computation of a surge cycle has to be done.

In 1975, Greitzer developed a 0D non-linear model based on performance map which predicts surge cycle with quite good agreement ((Greitzer, 1976-a) (Greitzer, 1976-b)). This model introduced a B parameter, which predicts the type of instability (rotating stall or surge) which will appear when mass flow is reduced. This model takes for granted that surge is a systemic instability and does not focus on blade geometry. In his work, N. Tauveron ((Tauveron N. L., 2006) (Tauveron N., 2007)) proposed a two-dimensional axisymmetric approach solving Euler equations with loss models for each blade rows. Correlations of head loss and deviation are used. These models describe quite well surge cycle and show which row is limiting, but cannot take into account 3D technological effects such as tip clearance effects for instance. Schöenborn (Schonenborn, 2004) uses a one-dimensional approach to make a vibration analysis. He had to estimate points of application for the resulting forces, which are different for every geometry. As a consequence, this method has to be confirmed by experiments. Three-dimensional models are necessary to take into account tip clearance effect, which may often induce surge precursors with strong consequences on vibration analysis (Niazi, 2000). Vahdati (Vahdati M., 2006) suggests a three-dimensional simulation of surge with one channel per row and a special boundary between rows allowing axial wave passage. This method is based on hypothesis that axial waves are much more energetic than circumferential waves. As a consequence, the method filters circumferential waves. With this method, great CPU time is saved, and most significant phenomena are present.

Mass flow inversion may occur in a surge configuration. Consequently, entrance of the domain can become an outlet of the domain. In (Vahdati M. , 2005), this problem is solved by using far-field boundary conditions, which are set to atmospheric conditions. Then, all the geometry of the engine has to be meshed. This is expensive, especially if the mesh has to be structured. Teramoto (Teramoto, 2008) presents a three-dimensional simulation of a surge cycle. All the geometry of the engine with an angular periodicity of 10° was meshed. That results in very high computation costs.

In the present paper, code coupling is used to simulate surge cycle of a compressor stage in a test bench facility. The originality of the method presented is that code coupling allows a systemic approach and an adequate treatment of compressor inlet and outlet boundary conditions which are difficult to determine during a computed surge phase. Indeed, at the boundaries of the 3D compressor domain, unsteady boundary conditions depending on the state of the fluid upstream and downstream of the compressor are imposed through the 1D-3D boundaries coupling described in the following numerical method description section. A 1D code computes aerodynamic field in parts of the system, upstream and downstream of the compressor in the test bench. Thus the system boundary conditions are set far enough from the compressor allowing pressure and mass flow waves to travel along the whole system.

The results presented here are the first steps of a study aiming at analysing the behaviour of 3.5 stages axial compressor during surge. Regarding the compressor behaviour observed at the moment when the test case for this study with one stage was chosen (Ottavy, Courtiade, & Gourdain, 2012), the last stage of this compressor seemed to be more unstable than the first one, for example. As going into deep surge was the main objective; that stage was chosen with the purpose to validate that deep surge cycle of a compressor may be described by the proposed 1D-3D coupling strategy.

1D-3D coupling has already been developed for internal combustion engines with methods of characteristics (Galindo, 2010). In that article, method of characteristic and fictive cells are used. Good agreement with analytical solution is found.

NUMERICAL METHOD

A coupling method between a 3D turbulent CFD code and a 1D CFD code with pressure losses models has been set up.

The idea of coupling is that 1D and 3D codes exchange adequate quantities at boundaries with a specific time period. The 1D and 3D aerodynamic fields are, therefore, synchronized during the unsteady computation allowing for example, the simulation of the propagation along the air flow line of a compression wave travelling from one end element of the system to the other end element. As a consequence, methodology of coupling depends on the treatment of boundaries for each code.

The software coupler Open-Palm developed by Cerfacs is used to deal with the boundary quantities exchanged via MPI processes ((Buis, 2006) (Piacenti, 2011)).

The Three-Dimensional Turbulent CFD Code

The 3D code used is elsA developed by ONERA (Cambier & Veuillot, 2008). The code solves the unsteady Reynolds Averaged Navier-Stokes equations with a finite volume approach on multiblock structured meshes. In this study, the convective fluxes are estimated with a third order upwind Roe scheme and the diffusive fluxes with a second order centered scheme. The time marching uses a Backward Euler integration scheme with an implicit phase using a scalar lower-upper symmetric successive over relaxation method (LUSSOR). The turbulent viscosity is computed with two equations model of Wilcox based on $k-\omega$ formulation (Wilcox, 1988).

At the inlet and outlet boundaries of the 3D computational domain, as the study also aims at following pressure waves travelling along the air flow line, the theory of characteristics is used: Euler equations are written as a system of waves carrying Riemann invariants along characteristic directions. The flow at each interfaces of the boundary is then determined by using local characteristic relations. Waves are classified as incoming or outgoing according to the sign of their velocity. If a wave is outgoing from the domain, the corresponding Riemann invariant is defined from the 3D domain. On the opposite, if a wave is incoming into the 3D domain, the corresponding Riemann invariant computed from the 1D solution has to be provided. With this treatment of the 1D-3D interfaces, there is no need to indicate the type of the boundary, inlet or outlet. This treatment done by the named "classical non reflexion" boundary condition available in the 3D code elsA, was the more appropriate to handle mass flow reversal. A complementary treatment is added to convert 0D data (from 1D side) into 2D data for the boundary conditions application on 3D side. By that way, effects of boundary layers or tangential gradients are then accounted.

On one side the coupling module exchanges with the 3D model mean values of conservative variables (ρ , ρV_x , ρV_y , ρV_z , ρE) on the boundary. Tangential velocities V_y and V_z are set to zero. Constant and uniform turbulent quantities are applied at coupling inlet boundaries during the computation. Of course, this turbulent treatment should be improved, but at this level of the model development, the basic treatment done allowed a full surge cycle simulation thus indicating that surge physic is dominated by mass flow and pressure waves. On the other side, the coupling module exchanges with the 1D model the quantities (P_s , T_s , V_x).

The One-Dimensional Eulerian CFD code

A one-dimensional modelling of the elements surrounding the compressor is used to simulate that part of the system in which 3D effects are not important; as a consequence, for those parts, we only take into account volumes and pressure losses. We have selected for that, the 1D software GT-Power, developed by Gamma Technologies, and which is widely used in the automobile industry.

GT-Power solves compressible 1D Euler equations on staggered grids. It is designed to simulate for example the air circuit of an automotive motor engine modelling the different elements of the system such as air filter, turbocharger, combustion chamber, heat exchanger, etc ... Those elements are modelled through the pressure losses they generate. Pressure losses are determined by classical empiric relations related to the specific geometrical element. A compressor or a turbine in a system is modelled for example by a pressure/mass flow operating map.

GT-Power includes User Routines, which allow the user to modify the system of equations solved by adding for example source terms or to modify the values of specified quantities during the computation. The User Routines are used in the present study to upgrade in time the boundary conditions imposed at the 1D/3D coupling boundary. The 3D domain and 1D domains have overlapping zones, which correspond to fictive cells for GT-Power domain, but to computational parts for elsA domain. GT-Power “fictive cells” option is used, which means that a fictive cell is added at the coupling end of the 1D domain. The values of static pressure, static temperature and velocity affected to that fictive cell through coupling data exchange, are extracted at the corresponding location in the 3D domain. GT-Power solver uses that fictive cell to compute the boundary condition to apply.

COUPLING METHOD VALIDATION ON AN ACADEMIC TEST CASE

Test Case Presentation

The case is composed of a rectangular cross section pipe, which is 9 meters long. This pipe is divided in three portions, which are respectively 4, 1 and 4 meters long. The flow in the short pipe in the middle is simulated with elsA and the two other pipe portions are simulated with GT-Power. This test case has two coupling boundaries between elsA and GT-Power, which could be alternatively an inlet or an outlet depending of the flow direction. The objectives of the test are to verify the good transmission of mass flow and pressure waves, and to validate that the numerical treatment done at the coupling boundaries can handle a mass flow reversal in the system. A stagnation pressure of 1 bar and a stagnation temperature of 288.6 K are imposed at inlet of the air pipe. Fig 1 shows the geometry of this test case.

Initialization is done with two computations without coupling (one for elsA and one for GT-Power) and a first coupling computation with constant pressure and temperature imposed at the extremities of the pipe. Convergence is checked through mass flow and pressure conservation in the entire domain.

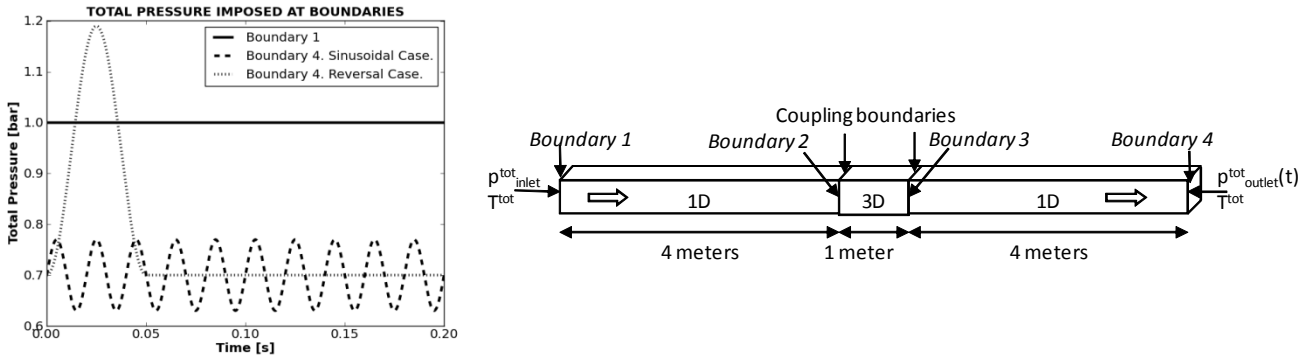


Fig 1: Academic test case geometry. Total pressure and total temperature imposed at inlet and outlet of the pipe for the sinusoidal case and the reversal case.

Two validation tests on this case are presented below.

In the first case, mass flow and energy conservation at coupling boundaries are evaluated. A sinusoidal total pressure signal represented on Fig 1 is imposed at the pipe outlet, boundary 4. Coupling boundaries will have to transfer sinusoid signals. Conservation of frequency and amplitude may be easily checked.

In the second case, a peak of outlet total pressure is imposed so that mass flow is reversed (Fig 1). Consequently, a coupling boundary which was an inlet (resp. outlet) for one of the code or pipe section becomes an outlet (resp. inlet). In order to avoid a strong reflection of waves on the pipe

inlet boundary, boundary 1, a 50 meters long pipe has been added upstream of the test configuration.

Tests on GT-Power show that results are better when a total pressure rather than a static pressure is imposed at an outlet.

Results

Sinusoidal Test Case

Fig 2 shows total pressure in a space-time diagram for the sinusoidal test case. It can be seen that the signal is not distorted at coupling boundaries, whose locations are marked with dotted lines. Relative difference of the conservative quantity ρE_t , ρ being the density and E_t total energy, is plotted in Fig 3. It appears that once periodic flow is established in the whole domain, after 0.12s, energy conservation is ensured with less than 1% of loss.

Figures Fig 4 and Fig 5 focus on mass flow behaviour at coupling boundaries. Shape of signal is well respected in term of frequency, while 20% of amplitude variation is observed. In Fig 5, the relative difference of mass flow is very weak for boundary 3. After 0.01 second, relative difference at boundary 2 is most of the time lower than 0.5%. But, when mass flow signal is at an extremum, relative difference may rise to 2% which is acceptable.

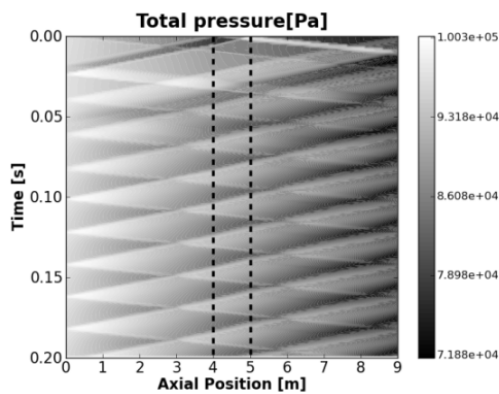


Fig 2: Space time evolution of total pressure for sinusoidal test case

Differences of total energy at boundaries 2 and 3

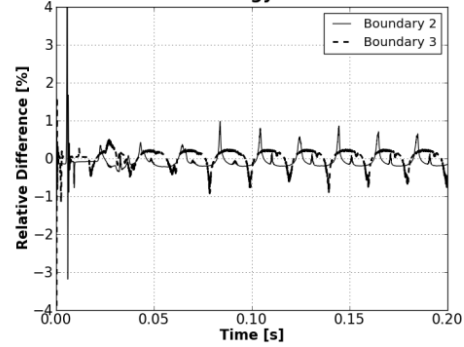


Fig 3: Total energy relative difference

between 1D and 3D sides

$$\left(\Delta(\rho E_{tot}) = \frac{\rho E_{tot}^{3D} - \rho E_{tot}^{1D}}{\rho E_{tot}^{3D}} \right)$$

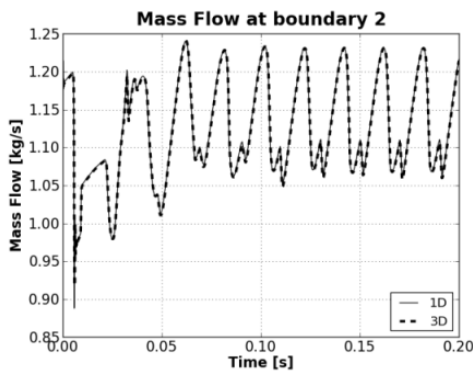


Fig 4: Mass flow at boundary 2 for 1D and 3D sides for sinusoidal test case.

Difference of mass flow at coupling boundaries

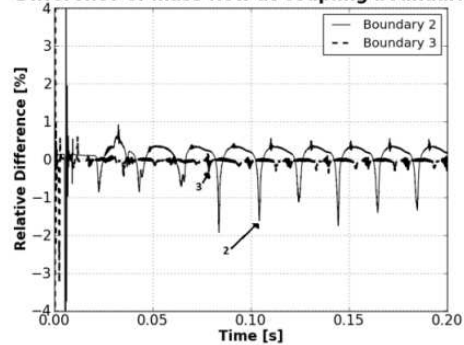


Fig 5: Mass flow relative difference between 1D and 3D sides.

On the whole, it appears that the coupling model produces less than 2% of loss of conservativity in mass flow and energy for sinusoidal signals without flow reversal.

Reversal Mass Flow Case

Fig 6 shows total pressure in a space-time diagram. The wave of higher pressure passes through the coupling boundaries. Fig 7 shows difference of total pressure divided by reference pressure of 75000 Pa at coupling boundaries. Differences are lower than 0.8% and rise as the pressure wave crosses the boundary.

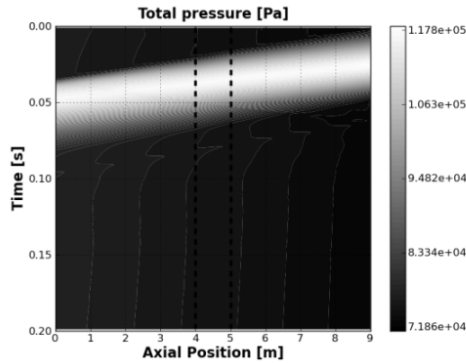


Fig 6: Space time evolution of total pressure for reversal mass flow test case.

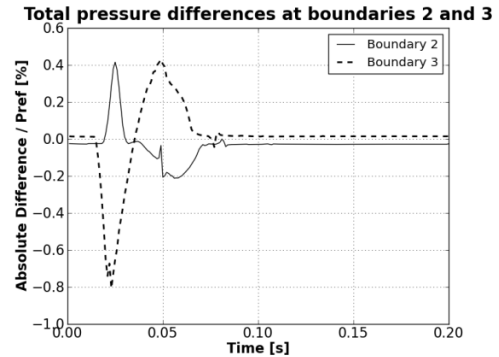


Fig 7: Total pressure difference
 $\left(dp_{tot} = \frac{p_{tot}^{3D} - p_{tot}^{1D}}{p_{tot}^{ref}}, p_{tot}^{ref} = 75000 Pa \right)$ between 1D and 3D.

Mass flow signals at coupling boundaries are given on Fig 8. GT-Power downstream peak of pressure signal reaches elsA downstream coupling boundary 3 on Fig 1 before the other elsA boundary 2. This explains the delay observed between the mass flow signals at the boundaries. At the end of the test, mass flow in the pipe stabilizes at 0.6 kg/s. Fig 9 shows that mass flow variation across a coupling boundary is lower than 2% of the converged value of the mass flow. At the end of the calculation, differences are lower than 0.25%. Mass flow reversal is correctly handled except close to zero mass flow value.

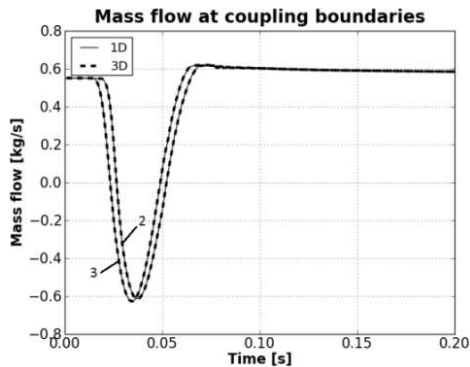


Fig 8: Mass flow at coupling boundaries for reversal mass flow test case. Boundaries are marked on figure 1.

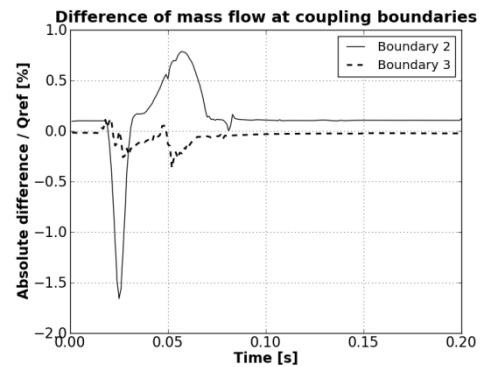


Fig 9: Mass flow difference at coupling boundaries divided by Qref=0.6 kg/s.

These tests validate the good behaviour at coupling boundaries. No signal distortion is observed and mass flow reversal is possible. The coupling method is then implemented on a configuration of a compressor stage in a test bench.

APPLICATION TO A SINGLE STAGE AXIAL FLOW COMPRESSOR

Description of Case

The fancied test bench studied in this paper is based on the 3½-stage compressor CREATE (Compresseur de Recherche pour l'Etude des effets Aerodynamiques et Technologiques, (Ottavy, Courtiade, & Gourdain, 2012)). CREATE is a high pressure compressor built by Snecma and tested at Ecole Centrale de Lyon in LMFA. The test rig is designed as an open loop. Upstream of the compressor, there is a throttle that decreases inlet total pressure and a settling chamber.

As explained earlier in this paper, for this first application of our coupling method to a more realistic turbomachinery case, the choice was done to restrict to the last stage of the compressor with the scope of reducing computation costs and draw the basic lines of what might be the scenario taking place in the complete machine. Of course, the effect of the missing stages is not accounted therefore comparisons with existing measurements cannot be done. This will be done in the next step where all 3½ stages of compressor CREATE will be simulated.

Preliminary Phase

A first step is to build the geometrical model of the test rig and of the compressor. For that, a steady characteristic of the third stage is computed with a classical steady approach with the 3D code elsA. Then, the 1D model of the test rig is built with GT-Power with the compressor characterized by its experimental performance map.

Steady Computation with elsA

Only one channel passage per row is simulated. A mixing plane boundary condition is used at stage boundary; it computes azimuthal average values of the conservative quantities at rows interface and transfer Riemann invariants through characteristic relations. On azimuthal boundaries, a periodic boundary condition is applied; this implies that the hypothesis of a periodic field is done. No azimuthal instability development is therefore allowed.

The mesh is generated with the turbomachinery grid generator Autogrid (Numeca International). A multi-domain approach is used with classical O-4H topology for each channel meshing. An O-grid is defined around the blade to allow an accurate description of the near-wall and leading edge regions. The construction of the mesh satisfies the constraint of a first cell next to the wall such that its height y^+ is acceptable for low Reynolds computations. A sensibility study on mesh has been done by (Ottavy, Courtiade, & Gourdain, 2012). The mesh has 634 785 nodes for rotor and 322 563 nodes for stator.



Fig 10: Geometry of 3D domain.

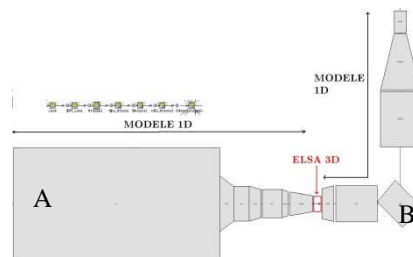


Fig 11: 1D-3D coupling model of CREATE

Stagnation pressure, stagnation temperature and flow angles are imposed at the inlet of the domain. This pressure and temperature are closed to experimental stagnation pressure and temperature at the inlet of the third stage in order to have similar Mach number between computational and experimental flows. At outlet, a valve law and a radial equilibrium are imposed. Adiabatic non-slip conditions are prescribed on the solid boundaries.

For these steady computations, convergence is observed through two criteria: a balance between the domain inlet and outlet mass flow at less than 1% and a minimum decrease of the equations residuals of two orders of magnitude.

The resulting steady characteristic, plotted in thick dark line, is presented in Fig 12.

Construction of GT-Power Model for Test Rig

GT-Power model of the test rig must correctly reproduce pressure losses in the circuit. For that, a first model of the experimental test rig with the experimental performance maps of the compressor has been built. Pressure losses in different parts of the model are tuned in order to get the correct nominal mass flow and pressure levels measured in the experiment. Steady characteristic of CREATE is recomputed by changing pressure loss coefficient of the valve downstream of the test rig.

Once the model is calibrated (pressure loss laws in different parts) on the compressor CREATE, stages not simulated by elsA are substituted by their equivalent volume and length. The rest of the model remains unchanged. Then, stagnation pressure and temperature imposed at inlet of GT-Power model (inlet of upstream plenum) are changed in order to get at the inlet of the third stage of the compressor simulated the same values in GT-Power and elsA models. Thus, at the beginning of surge cycle, the pressure at the inlet of the compressor stage simulated has a pressure level close to the pressure measured at inlet of third stage of compressor CREATE. The model of the test rig for the configuration presented in this article is then built.

Coupling Computations

Coupling computations are set up. The time step is defined as a fraction of the time period of the propagation of an axial wave from one end of the test rig to the other. The wave velocity considered is the nominal velocity on the steady characteristic. Time steps dt_1 and dt_2 , used for the surge cycles computations are such that the time period is discretized with 5500 instants and 11000 instants, respectively. The period of the surge cycle computed is therefore discretized with almost 4500 instants with dt_1 . Exchanges of information between elsA and GT-Power append every $5*dt_1$ and $10*dt_2$. The computation cost of one cycle with dt_1 is about 33h with 60 MPI tasks for the 3D computation.

Performance Map

The steady characteristic of the 1D-3D model is obtained by changing pressure loss coefficient of downstream valve. A surge cycle is started when this pressure loss coefficient is too high and no steady solution can be obtained. Fig 12 shows characteristic obtained for steady computations with elsA alone (“w/o coupling” data) or coupled with GT-Power (“coupling” data). The trajectory of instantaneous performance of compressor during a surge cycle is also plotted (“surge” data). In figures Fig 12 and Fig 13, subscript ref relates to mass flow and pressure ratio at nominal point of characteristic computed without any coupling. Time is divided by the time period of the surge cycle.

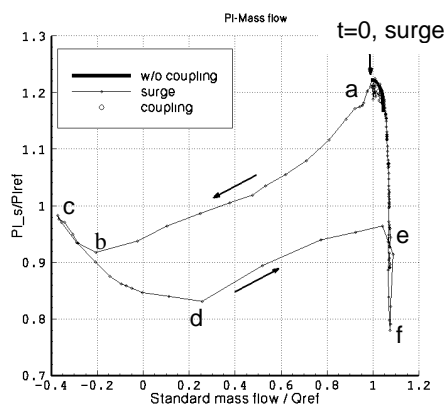


Fig 12: Performance map of the compressor for steady computations with or without coupling and surge cycle with dt_1 .

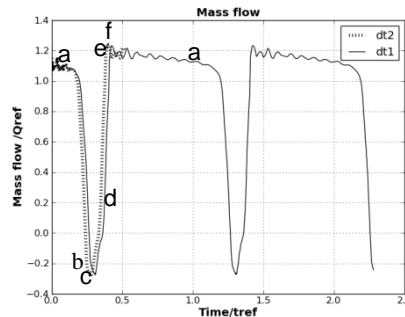


Fig 13: Instantaneous mass flow in compressor during surge cycle for two time steps.

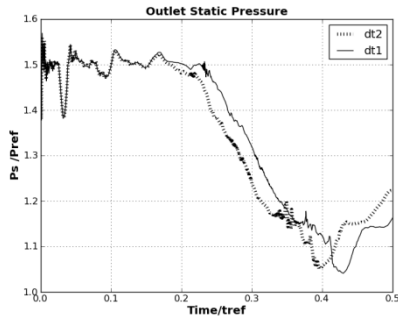


Fig 14: Instantaneous static pressure at the outlet of the compressor.

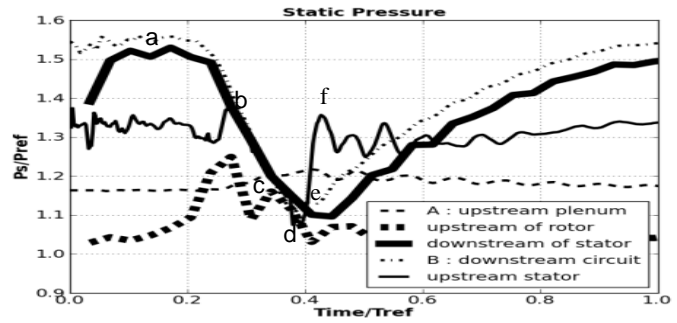


Fig 15: Instantaneous static pressure at the inlet and outlet of the compressor (cycle with dt_1). Positions A and B in test bench are explained at Fig 11.

Surge cycles are similar for the two time steps presented. The only difference observed is that the surge cycle starts earlier for the smaller time step. However, it can be seen in Fig 14 that no significant modification of the signals appears when the time step is reduced. So, all the detailed analysis is done with the results obtained with the higher time step. It appears that several identical deep surge cycles are computed (Fig 13 and Fig 15) with a mass flow clearly reversed during part of the surge. Performance map focuses on one of the cycles. The trajectory of the surge cycle is very close to the coupled steady characteristic (labelled “coupling” on Fig 12) for high mass flows. However, in the high mass flow part of the performance curve (Fig 12), the pressure ratio in the elsA model alone is slightly higher than for the 1D-3D coupled model which accounts for the losses in the 1D parts. In Fig 12, on surge trajectory, filled circle symbols are uniformly distributed in time; as the symbols are more concentrated for high mass flow, we deduce that most of the surge cycle occurs in high mass flows region.

From (a) to (b), mass flow and pressure ratio decrease until static pressure downstream of the stator is equal to static pressure upstream of stator. From (b) to (c), static pressure decreases in all compressor. But, negative mass flow increase, and since compressor works as a turbine, pressure ratio rises. A minimum reversed mass flow and maximum pressure ratio is reached at (c). Then, as the pressure upstream of the rotor in the test bench has increased (upstream volumes are filling), the pressure just upstream of the rotor increases as well. At the same time, the pressure around the stator is still decreasing (downstream volumes are emptying), therefore, pressure ratio decrease. Zero mass flow point is reached and mass flow returns to positive value. The pressure ratio is minimum at (d). At point (d), local aerodynamic of rotor is improved and, therefore, pressure ratio may increase again. From (d) to (e), mass flow increases until maximum mass flow at the sonic blockage in the rotor and stator. At that maximum positive mass flow, most of the energy brought to the fluid by the rotor is converted into pressure. But, on the contrary, as pressure is still decreasing downstream the stator, the pressure level there becomes lower than the pressure at rotor exit. The stator is working as a “turbine stator”; the rotor is choked. As a consequence the stage pressure ratio drops from (e) to (f). Then, the pressure at the stator exit starts to increase again and from (f) to (a) pressure ratio rises, the system downstream the compressor repressurises.

Aerodynamic field

In Figure 16, the plane located at a fixed axial position at mid-chord of the rotor channel is coloured by the entropy field for different times indicated on the small mass flow time diagrams. Lower entropy is represented by a darker colour. Two dark contours of axial velocity are added to the figure. The thick dark line represents zero axial velocity and the thin dark line the slightly positive axial velocity.

At the beginning of surge cycle, axial velocity is reversed only in the tip clearance gap zone close to the blade suction side (where entropy is also higher). This flow reversion is induced by the

tip clearance jet and the related vortex occurring across the tip clearance gap at the rotor blade extremity (a). As the time increases, the reversion zone extends in the circumferential direction and covers the whole gap between the pressure side and suction side of the blade channel, covering the whole region close to the casing (b). When mass flow decreases again, the reversion zone extends toward the hub and entropy rises in the entire channel (c). When mass flow is globally reversed (d-e-f), entropy is still high. At the beginning of this time region, axial velocity stays positive on the pressure side of blades (d). However, at minimum mass flow, axial velocity is positive only in the tip clearance zone and close to the hub (e). At the end of the negative mass flow time, the positive zone at hub extends toward pressure side (f). As a consequence, mass flow rises again. Then, positive zone of axial velocity increases from shroud until tip clearance area (g). Once, the whole channel (except tip clearance area) has positive axial velocity, entropy reduces (h).

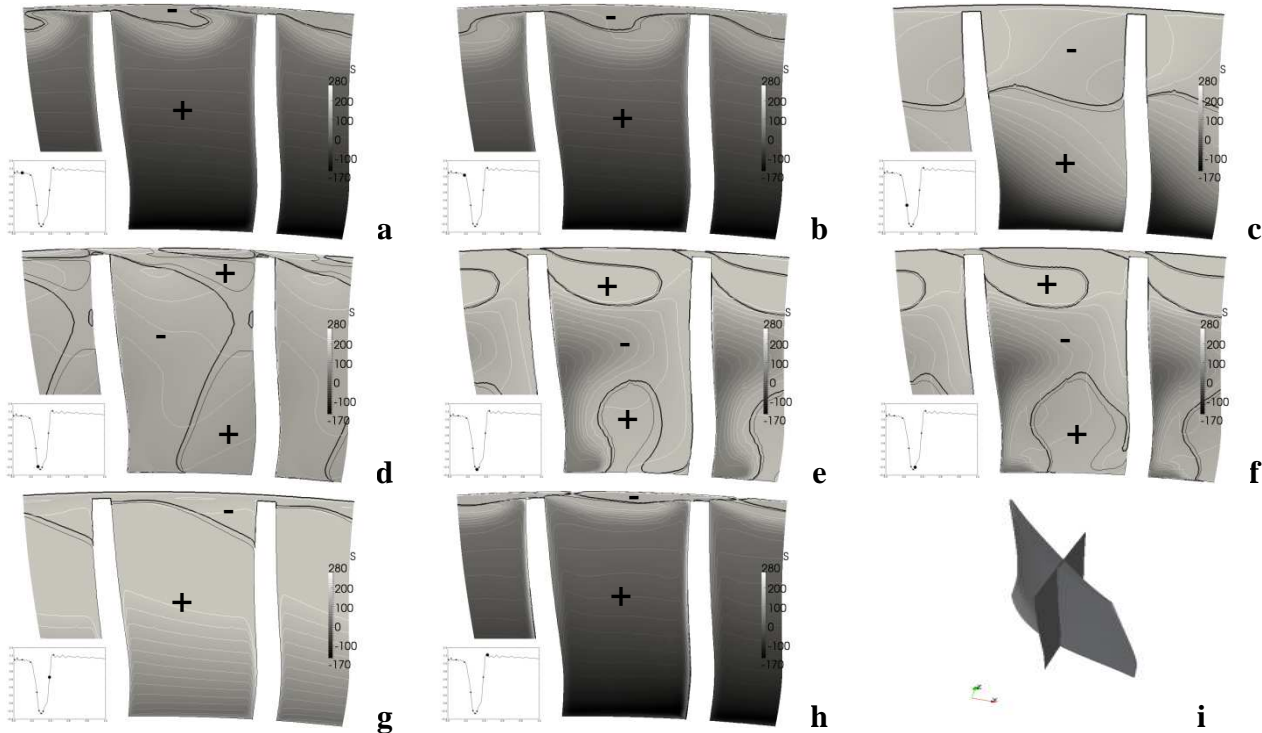


Figure 16: Entropy field in an axial plane at mid-chord of the rotor and at different instants during the surge cycle. Black dots on the small mass flow-time diagrams locate the instant in the cycle. The axial plane location is presented on figure (i). Contours of zero axial velocity (thick dark line) and slightly positive axial velocity (thin dark line) are drawn.

CONCLUSIONS

A 1D-3D coupling methodology has been set up in order to study systemic instabilities of compressor stage. The surge cycle computed with this new tool gives very interesting information on time characteristic curves and mass flow evolution. The 3D aerodynamic field has been analysed during the surge cycle, enlightening the importance of tip clearance flow on mass flow evolution.

Access to the time evolutions of the 3D local quantities during a surge cycle and flow figures inside the compressor is clearly an advantage of this new method. Moreover, this numerical simulation performed with a very reasonable computation cost, could provide valuable information to the designers; for instance, for the estimation of the blade forces during surge.

In further study, all stages of compressor CREATE will be simulated.

ACKNOWLEDGEMENTS

The authors wish to acknowledge the company Snecma (SAFRAN) which supports the PhD of Florence de Crécy and the company Renault which supports the PhD of Guillaume Desprès.

We also wish to thank Gamma Technology, Cerfacs and Onera for software support and IDRIS, the CNRS's national supercomputing center where some of the computations have been performed.

REFERENCES

- Buis, S., Piacentini, A., & Déclat, D. (2006). PALM: A Computational framework for assembling high performance computing applications. *Concurrency Computat.: Pract. Exper.* , Vol18(2),p 247-262.
- Cambier, L., & Veuillot, J. (2008). Status of the elsA CFD software for flow simulation and multidisciplinary applications. *46th AIAA Aerospace Sciences Meeting and Exhibit*. Reno, Nevada.
- Courtiade, N., Ottavy, X., & Gourdain, N. (2011). Experimental investigation of rotating stall in a high speed multi-stage axial compressor. *9th European Turbomachinery Conference*. Istanbul, Turkey.
- di Mare, L. (2009). Aerodynamics and elasticity of a compressor during surge and reversed flow. *12th ISUAAAT*. London, UK.
- Galindo, J., Tiseira, A., Fajardo, P., & Navarro, R. (2010). Coupling methodology of 1d finite difference and 3d finite volumes cfd codes based on the method of characteristics. *Mathematical and Computer Modelling* .
- Gourdain, N., Burguburu, S., Leboeuf, F., & Miton, H. (2006). Numerical simulation of rotating stall in a subsonic compressor. *Aerospace Science and Technology* , 9-18.
- Greitzer, E. (1976-a). Surge and rotating stall in axial flow compressors, Part I: Theoretical compression system model. *Journal of Engineering for Power* , 190-198.
- Greitzer, E. (1976-b). Surge and Rotating Stall in Axial Flow Compressors—Part II: Experimental Results and Comparison With Theory. *Journal of Engineering for Power* , 199-211.
- Niazi, S. (2000). Numerical simulation of rotating stall and surge alleviation in axial compressors. USA: PhD thesis, Georgia Institute of Technology, Department of aerospace engineering.
- Ottavy, X., Courtiade, N., & Gourdain, N. (2012). Experimental and Computational Methods for Flow Investigation in High-Speed Multistage Compressor. *Journal of Propulsion and Power* , 1141-1155.
- Piacenti, A., Morel, T., Thévenin, A., & Duchaine, F. (2011). Open-PALM: an Open Source Dynamic Parallel Coupler. *In Coupled Problems*. Kos Island, Greece.
- Schonenborn, H., & Breuer, T. (2004). Aerodynamic and Mechanical Vibration Analysis of a Compressor Blisk at Surge. *ASME* .
- Tauveron, N., Leboeuf, F., & Ferrand, P. (2006). Dynamic Modeling of a Nuclear Gas Turbine Plant: Application to Surge Prediction. *ASME* .
- Tauveron, N., Saez, M., Ferrand, P., & Leboeuf, F. (2007). Axial turbomachine modelling with a 1D axisymmetric approach: Application to gas cooled nuclear reactor. *Nuclear Engineering and Design* , 1679-1692.
- Teramoto, S. (2008). Analysis of the entire surge cycle of a multi-stage high-speed compressor. *Annual Research Briefs* , 205-218.
- Vahdati, M., Sayma, A., Freeman, C., & Imregun, M. (2005). On the use of atmospheric boundary conditions for axial-flow compressor stall simulations. *Journal of Turbomachinery* , 349.
- Vahdati, M., Simpson, G., & Imregun, M. (2006). Unsteady flow and aeroelasticity behaviour of aero engine core compressors during rotating stall and surge". *ASME* .
- Wilcox, D. (1988). Reassessment of the Scale Determining Equation for Advanced Turbulence Models. *AIAA J.* , 1299-1310.